2 Radar Basics

This chapter explains the fundamental concepts of chirp sequence radars. A short introduction is given in the beginning, followed by an explanation of its functionality, and an explanation for signal processing used in unmodulated Continous wave Radars. Later, Frequency Modulated Continuous Wave Radars are presented and analyzed starting with a simple single chirp modulation. Finally, the Chirp-Sequence modulation is shown, and the signal processing chain, to obtain the range and velocity of a target, is explained.

The term RADAR stands for **RA**dio **D**etection **A**nd **RA**nging. The primary task of radars is to search and identify true targets by the transmission of electromagnetic signals into a specific volume of space. The reflection of the transmitted signals on the objects (targets) produce echoes in the direction of the radar. Then, the received echoes are processed by the radar receiver in order to estimate characteristics of the target such as range, radial velocity, and azimuth angle.

The history of radars starts in the year of 1904 when engineer Christian Hülsmeyer invented and fabricated the first radar to detect ships in difficult weather conditions, and avoid collisions. Although the invention did not get financial support, research in the field of radar technology continued. Significant progress was achieved during the Second World War in military applications related to detection of ships and aircrafts [1].

In the recent years, the development of small radars has been possible due to the advance of microwave technology and signal processing. These improvements have allowed the design of more complex systems that can identify multiple targets, and estimate the angular position of those targets, for example in automotive applications. Currently, automotive applications provide an interesting field of research focused on adaptive cruise control (ACC) systems, Intelligent Drive and safety applications such as blind spot surveillance, pre-crash recognition, and collision avoidance [1].

2.1 Radar Classification

Depending on the signal used for transmission, radars can be classified into pulsed and Continuous Wave (CW). In the first case, the transmitted signal consists of time-limited pulsed waveforms. CW radars transmit a continuous waveform that can be considered as a sinusoidal signal in the form of $\cos(2\pi f_{\mathrm{T}} t)$.

CW radars can be further classified into unmodulated Continuous Wave radars and Frequency Modulated Continuous Wave (FMCW) radars. The information of the target's velocity can be extracted from the analysis of an unmodulated CW radar, while the range cannot be uniquely identified. To estimate the range, the variation of frequency of the transmitted signal as a function of time can be introduced through the FMCW radar concept.

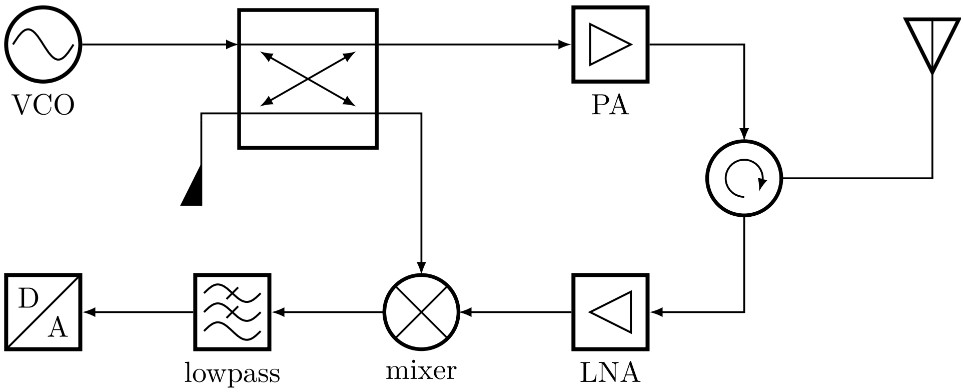

Fig. 2.1: Simplified block diagram of CW radar.

2.2 Unmodulated Continuous Wave Radars

Unmodulated CW radars can accurately measure the target's radial velocity by using the so called Doppler shift. Moreover, the angular position of the target can also be estimated if more than one receiver antenna is used. In contrast, the target range cannot be uniquely measured using a simple unmodulated CW radar.

Fig. 2.1 shows the general block diagram of a simplified unmodulated CW radar sensor [2]. An oscillator creates a sinusoidal wave in the form of $\cos(2\pi f_\mathrm{T} t)$ with constant frequency $f_\mathrm{T} = f_\mathrm{c}$. The sinusoidal wave is fed into to a directional coupler in order to perform power division. Part of the power flows through a circulator, and the signal is radiated into the space by a transmitter antenna. Later on, an echo is produced by the reflection of the radiated signal on the targets and clutter (unwanted background reflectors). Then, the echo signal is received by an antenna or a uniform linear array of antennas. The received signal passes through a Low Noise Amplifier (LNA) and is mixed with the original transmitted signal. Next, a low pass filter (LP) is applied in order to keep the low frequency intermodulation products. Then the signal is applied to an analog to digital converter (ADC) for further processing.

In the simplest case of a stationary target, the generated echoes are captured by the receiver antenna and the spectrum of the received echoes is concentrated around f_c. On the other hand, if the target is moving, the spectrum is shifted by the Doppler frequency f_D. Then, the target radial velocity can be easily estimated by the measurement of the Doppler frequency [3].

In order to understand how the velocity can be measured, taking into account the relation between frequency and phase

$$\frac{d\varphi(t)}{dt} = \omega = 2\pi f, \tag{2.1}$$

it is possible to assume that the transmitted signal is

$$s_\mathrm{T}(t) = A_\mathrm{T}\cos(2\pi f_\mathrm{T} t) = A_\mathrm{T}\cos(2\pi f_\mathrm{c} t) = A_\mathrm{T}\cos(\varphi_\mathrm{T}(t)). \tag{2.2}$$

where A_T is the amplitude of the transmitted signal.

The received target echo signal $s_\mathrm{R}(t)$ is a reflected, attenuated, and delayed copy of the transmitted signal $s_\mathrm{T}(t)$. Calling R the distance between radar and target at the initial position, v the velocity at which the target moves, and assuming that the echo travels with the speed of light c, the delay τ is directly proportional to the round trip distance $2R$ the echo travels between radar and target, plus the distance $2(vt)$ the target travels during time t.

$$\tau = \frac{2}{c}(R + vt) \tag{2.3}$$

Then, the received signal with attenuated amplitude A_R is

$$s_\mathrm{R}(t) = A_\mathrm{R}\cos(2\pi f_\mathrm{c}(t-\tau)) = A_\mathrm{R}\cos(\varphi_\mathrm{T}(t-\tau)) = A_\mathrm{R}\cos(\varphi_\mathrm{R}(t)). \tag{2.4}$$

It can be seen that the substitution of (2.3) into (2.4) gives as a result an expression of the received signal containing the information of the Doppler frequency f_D, and a constant phase term φ_R that depends on the range R.

$$s_\mathrm{R}(t) = A_\mathrm{R}\cos\left[2\pi\left(f_\mathrm{c} - \underbrace{\frac{2f_\mathrm{c}vt}{c}}_{f_\mathrm{D}}\right)t - \underbrace{2\pi f_\mathrm{c}\frac{2R}{c}}_{\varphi_\mathrm{R}}\right] \tag{2.5}$$

Later, the transmitted and received signals are mixed and filtered in order to keep the low frequency intermodulation products

$$\begin{aligned} s_\mathrm{T}(t)s_\mathrm{R}(t) &= A_\mathrm{T}\cos(\varphi_\mathrm{T}(t))\ A_\mathrm{R}\cos(\varphi_\mathrm{R}(t)) \\ &= \frac{A_\mathrm{T}A_\mathrm{R}}{2}[\cos(\varphi_\mathrm{T}(t)+\varphi_\mathrm{R}(t)) + \cos(\varphi_\mathrm{T}(t)-\varphi_\mathrm{R}(t))]. \end{aligned} \tag{2.6}$$

Hence, the phase of the real-valued intermediate frequency signal $s_\mathrm{IF}(t) = A_\mathrm{IF}\cos(\Delta\varphi(t))$ is

$$\begin{aligned} \Delta\varphi(t) &= \varphi_\mathrm{T}(t) - \varphi_\mathrm{R}(t) = \varphi_\mathrm{T}(t) - \varphi_\mathrm{T}(t-\tau) = 2\pi f_\mathrm{c}t - 2\pi f_\mathrm{c}(t-\tau) \\ &= 2\pi f_\mathrm{c}\tau = 2\pi\underbrace{\frac{2f_\mathrm{c}v}{c}}_{f_\mathrm{D}}t + \underbrace{2\pi f_\mathrm{c}\frac{2R}{c}}_{\varphi_\mathrm{R}}. \end{aligned} \tag{2.7}$$

Thereby, if the Doppler frequency f_D is measured, the velocity of the target can be estimated by

$$v = \frac{f_\mathrm{D}}{2}\frac{c}{f_\mathrm{c}} = \frac{f_\mathrm{D}}{2}\lambda. \tag{2.8}$$

2.3 Frequency Modulated Continuous Wave Radars

FMCW radars are commonly used today due to the fact that high circuit integration can be achieved using MMICs (Monolithic Microwave Integrated Circuits) [2]. These kind of radars can measure not only the target velocity, but also the range. This is done by modulation of frequency f_T of the transmitted signal $\cos(2\pi f_\mathrm{T}t)$. Just like unmodulated CW radars, the FMCW radar can measure the angular position of a target if an array of antennas is used at the receiver, instead of a single antenna.

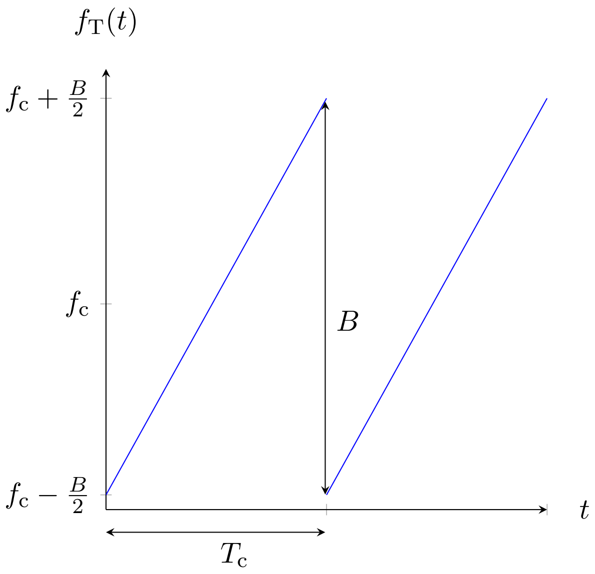

(a) Frequency of sawtooth modulated signal.

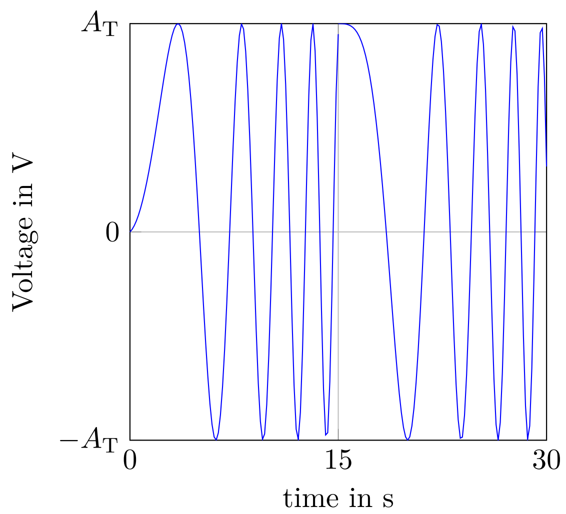

(b) Transmitted signals using sawtooth modulation.

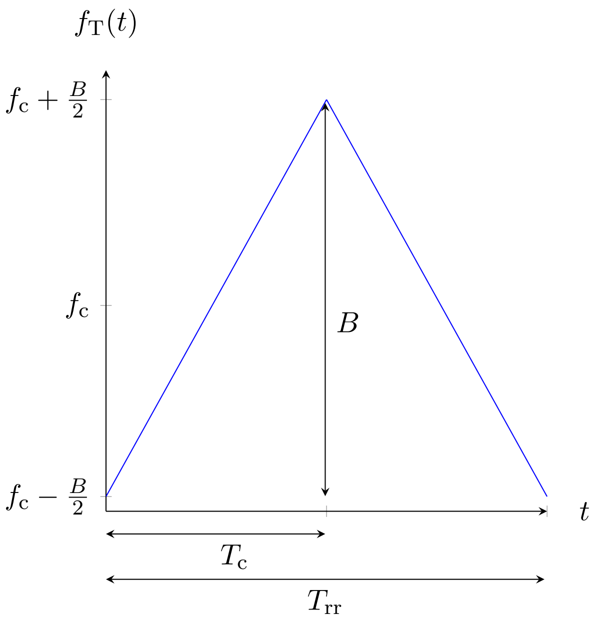

(c) Frequency of triangular modulated signal.

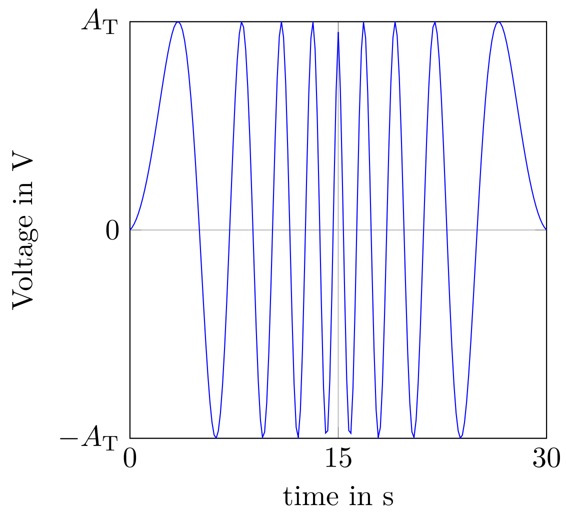

(d) Transmitted signal using triangular modulation.

Fig. 2.2: FMCW transmitted signal $\cos(2\pi f_T(t)t)$ using sawtooth (up) and triangular (down) modulations.

Unlike an unmodulated CW radar, the generator of the transmitted signal in a FMCW radar is not a simple VCO (Voltage Controlled Oscillator), but a generator which creates frequency modulated sinusoidal signals. The most common modulation approaches used for automotive applications are sawtooth and triangular modulation.

Fig. 2.2 shows the possible modulations schemes. In the fist case, the sinusoidal signal is linearly modulated using a frequency ramp with bandwidth B, duration T_c, and carrier frequency

f_c. The frequency of two transmitted ramps is depicted in Fig. 2.2 (a) and the transmitted signals can be seen in Fig. 2.2 (b). In the second case, the sinusoidal signal is linearly modulated using a frequency ramp with positive slope and another with negative slope with total duration T_rr. As can be seen in Fig. 2.2 (c), each ramp has a bandwidth B, duration T_c, and carrier frequency f_c. An example of this type of transmitted signal is shown in Fig. 2.2 (d).

2.3.1 Single Chirp Modulation

When the ramps used in the sawtooth modulation are very steep, they can be called chirps. The variation of frequency in time of a chirp signal can be described by

$$f_\mathrm{T}(t) = f_\mathrm{c} + \frac{B}{T_\mathrm{c}}t,\ t \in \left[\frac{-T_\mathrm{c}}{2}, \frac{T_\mathrm{c}}{2}\right]. \tag{2.9}$$

Taking into account (2.1), the phase of the transmitted signal $s_\mathrm{T}(t) = A_\mathrm{T}\cos(\varphi_\mathrm{T}(t))$ is

$$\begin{aligned}\varphi_\mathrm{T}(t) &= 2\pi\int_{-\frac{T}{2}}^{t} f_\mathrm{T}(t)\mathrm{d}t = 2\pi\left(f_\mathrm{c}t + \frac{1}{2}\frac{B}{T_\mathrm{c}}t^2\right) - 2\pi\left(-f_\mathrm{c}\frac{T}{2} + \frac{1}{8}B\frac{T^2}{T_\mathrm{c}}\right)\\ &= 2\pi\left(f_\mathrm{c}t + \frac{1}{2}\frac{B}{T_\mathrm{c}}t^2\right) - \varphi_\mathrm{T0}\end{aligned} \tag{2.10}$$

and the phase of the received echo signal $s_\mathrm{R}(t) = A_\mathrm{R}\cos(\varphi_\mathrm{R}(t))$ is

$$\begin{aligned}\varphi_\mathrm{R}(t) = \varphi_\mathrm{T}(t-\tau) &= 2\pi\left(f_\mathrm{c}(t-\tau) + \frac{1}{2}\frac{B}{T_\mathrm{c}}(t-\tau)^2\right) - \varphi_\mathrm{T0}\\ &= 2\pi\left(f_\mathrm{c}t - f_\mathrm{c}\tau + \frac{1}{2}\frac{B}{T_\mathrm{c}}t^2 - \frac{B}{T_\mathrm{c}}\tau t + \frac{1}{2}\frac{B}{T_\mathrm{c}}\tau^2\right) - \varphi_\mathrm{T0}.\end{aligned} \tag{2.11}$$

After mixing and filtering, the phase of the real-valued intermediate frequency signal $s_\mathrm{IF}(t) = A_\mathrm{IF}\cos(\Delta\varphi(t))$ is

$$\begin{aligned}\Delta\varphi(t) = \varphi_\mathrm{T}(t) - \varphi_\mathrm{R}(t) &= 2\pi\left(f_\mathrm{c}\tau + \frac{B}{T_\mathrm{c}}\tau t - \underbrace{\frac{1}{2}\frac{B}{T_\mathrm{c}}\tau^2}_{\ll 1}\right)\\ &= 2\pi\left(f_\mathrm{c}\tau + \frac{B}{T_\mathrm{c}}\tau t\right),\end{aligned} \tag{2.12}$$

where the third term can be neglected due to the fact that $\tau \ll T_\mathrm{c}$. Substituting τ from (2.3) in (2.12), result as

$$\begin{aligned}\Delta\varphi(t) &= 2\pi\left(\frac{2f_\mathrm{c}R}{c} + \frac{2f_\mathrm{c}v}{c}t + \frac{2R}{c}\frac{B}{T_\mathrm{c}}t + \underbrace{\frac{2v}{c}\frac{B}{T_\mathrm{c}}t^2}_{\substack{\text{Range Doppler}\\ \text{Coupling}}}\right)\\ &\approx 2\pi\left(\frac{2f_\mathrm{c}R}{c} + \left(\frac{2f_\mathrm{c}v}{c} + \frac{2R}{c}\frac{B}{T_\mathrm{c}}\right)t\right).\end{aligned} \tag{2.13}$$

The last term of (2.13) is called Range Doppler Coupling, and can be neglected as it is small compared to the other terms [4].

The frequency associated with the intermediate frequency signal $s_{\mathrm{IF}}(t)$ can be obtained from phase $\Delta\varphi(t)$ using (2.1). This is the so called beat frequency f_{B}, which analytically is represented by a velocity related frequency component f_{D} (Doppler frequency), and a range related frequency component f_{R} (range frequency)

$$\begin{aligned} f_{\mathrm{B}} &= \frac{1}{2\pi}\frac{d\Delta\varphi(t)}{dt} = \frac{2R}{c}\frac{B}{T_{\mathrm{c}}} + \frac{2f_{\mathrm{c}}v}{c} \\ &= \underbrace{\frac{2R}{c}\frac{B}{T_{\mathrm{c}}}}_{f_{\mathrm{R}}} - \left(\underbrace{-\frac{2f_{\mathrm{c}}v}{c}}_{f_{\mathrm{D}}}\right). \end{aligned} \tag{2.14}$$

Consequently, the velocity can be estimated if the Doppler frequency f_{D} is measured using (2.8) and the target velocity can be estimated from the range frequency

$$R = \frac{c}{2}\frac{T_{\mathrm{c}}}{B} f_{\mathrm{R}}. \tag{2.15}$$

Fig. 2.3 shows a simple graphic representation of the mentioned frequencies for the case when two ideal chirps are transmitted. The frequency of the transmitted signal is depicted in blue, the frequency of a received signal corresponding to a static target is red, and the frequency related to a moving target is green. In the simplest case of a static target (red), the received signal is delayed by τ, stays within bandwidth B, and the velocity related term in equation (2.14) is zero ($f_{\mathrm{D}} = 0$). This means that the beat frequency f_{B} is equal to the range frequency f_{R}. On the other hand, if the target is moving (green), the received signal is also a delayed version by τ, but a frequency shift of f_{D} is introduced. Then, the beat frequency f_{B} comprises the range frequency f_{R} and the Doppler frequency f_{D}.

The analytic intermediate frequency signal can be calculated by

$$\begin{aligned} s_{\mathrm{IF_a}}(t) &= s_{\mathrm{IF}}(t) + i\,\mathcal{H}\{s_{\mathrm{IF}}(t)\} = A_{\mathrm{IF}}\cos(\Delta\varphi(t)) + i\,A_{\mathrm{IF}}\sin(\Delta\varphi(t)) = A_{\mathrm{IF}}\,e^{i\Delta\varphi(t)} \\ &= A_{\mathrm{IF}}\,e^{i2\pi\left[\frac{2f_{\mathrm{c}}R}{c} + \left(\frac{2f_{\mathrm{c}}v}{c} + \frac{2R}{c}\frac{B}{T_{\mathrm{c}}}\right)t\right]}, \end{aligned} \tag{2.16}$$

where $\mathcal{H}\{s_{\mathrm{IF}}(t)\}$ denotes the Hilbert transform of the real-valued signal $s_{\mathrm{IF}}(t)$. Finally, a window function $w(t)$ can be applied giving as a result the analytic intermediate frequency signal

$$s_{\mathrm{IF_a}}(t) = A_{\mathrm{IF}}\,e^{i2\pi\left[\frac{2f_{\mathrm{c}}R}{c} + \left(\frac{2f_{\mathrm{c}}v}{c} + \frac{2R}{c}\frac{B}{T_{\mathrm{c}}}\right)t\right]} \cdot w(t). \tag{2.17}$$

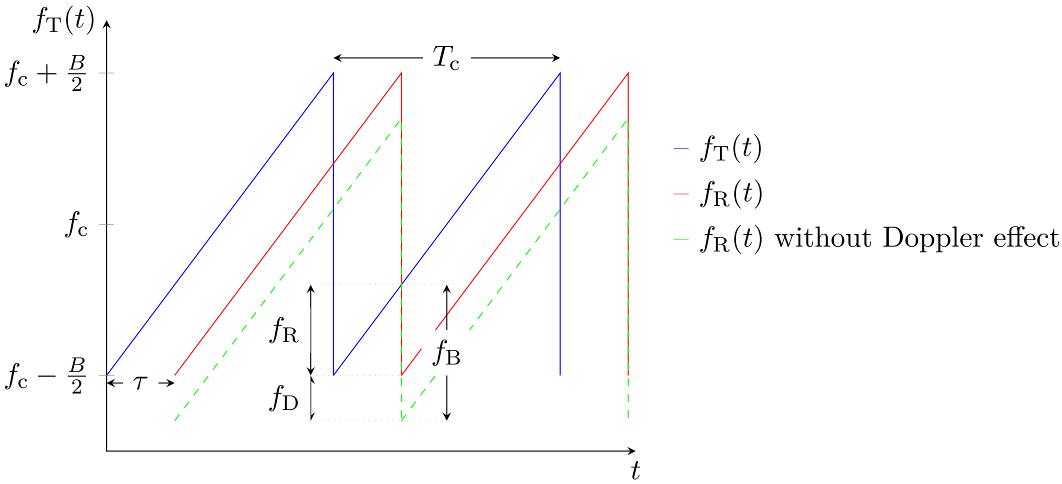

Fig. 2.3: Graphical description of the beat frequency for one target static (red) and one moving target (green).

2.3.2 Chirp-Sequence Modulation

In the past, the generation of fast linear frequency ramps with large baseband bandwidths presented to be a problem. Nowadays, it is possible due to recent development in integrated PLLs and fast circuits [2]. However, in a real chrip-sequence transmission, once a ramp is generated, a short idle time, determined by the ramp down settling time, is needed to start a new chirp. Therefore, the chirp repetition time T_r is defined. Fig. 2.4 depicts a chirp frequency modulation where L frequency ramps with constant ramp duration T_c and ramp repetition period T_r are transmitted.

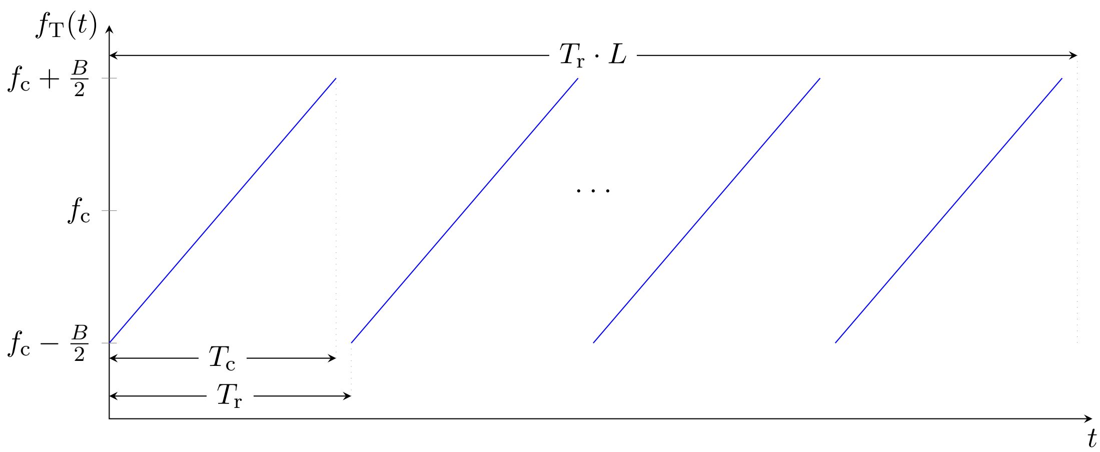

Fig. 2.4: Sketch of chirp-sequence modulation.

Then, the variable R is redefined for each chirp using $R + vT_rl$ with $l \in \{0, 1, 2, ..., L - 1\}$.

Rewriting (2.17) , the analytic intermediate frequency signal can be represented as

$$
\begin{aligned}
s_{\mathrm{IF_a,2D}}(t) &= A_{\mathrm{IF}} \sum_{l=0}^{L-1} e^{i2\pi\left[\frac{2f_c(R+vT_r l)}{c}+\left(\frac{2f_c v}{c}+\frac{2(R+vT_r l)}{c}\frac{B}{T_c}\right)t\right]} \cdot \mathrm{rect}\left(\frac{t-l\cdot T_r}{T_c}\right) \\
&= A_{\mathrm{IF}}\, e^{i2\pi\frac{2f_c R}{c}} \sum_{l=0}^{L-1} e^{i2\pi\left[\frac{2f_c vT_r l}{c}+\left(\frac{2f_c v}{c}+\frac{2RB}{c\cdot T_c}+\frac{2BvT_r l}{c\cdot T_c}\right)t\right]} \cdot \mathrm{rect}\left(\frac{t-l\cdot T_r}{T_c}\right) \\
&\approx A_{\mathrm{IF}}\, e^{i2\pi\frac{2f_c R}{c}} \sum_{l=0}^{L-1} e^{i2\pi\left[\frac{2f_c vT_r l}{c}+\left(\frac{2f_c v}{c}+\frac{2RB}{c\cdot T_c}\right)t\right]} \cdot \mathrm{rect}\left(\frac{t-l\cdot T_r}{T_c}\right),
\end{aligned}
\tag{2.18}
$$

where the last term $\frac{2BvT_r l}{c\cdot T_c}$ has been neglected as it is small compared to the other terms [4].

Later, the signal is sampled with sampling frequency $f_s(n) = \frac{1}{T_s}$ and $n \in \{0, 1, 2, ..., N-1\}$ during each ramp giving as a result

$$
\begin{aligned}
s_{\mathrm{IF_a,2D}}(n,l) &= A_{\mathrm{IF}}\, e^{i2\pi\frac{2f_c R}{c}} \sum_{l=0}^{L-1}\sum_{n=0}^{N-1} e^{i2\pi\left[\frac{2f_c vT_r l}{c}+\left(\frac{2f_c v}{c}+\frac{2RB}{c\cdot T_c}\right)nT_s\right]}, \\
&= A_{\mathrm{IF}}\, e^{i2\pi\frac{2f_c R}{c}} \left[\sum_{l=0}^{L-1} e^{i2\pi\left(\frac{2f_c vT_r}{c}\right)l} \left[\sum_{n=0}^{N-1} e^{i2\pi\left(\frac{2f_c v}{c}+\frac{2RB}{c\cdot T_c}\right)nT_s}\right]\right].
\end{aligned}
\tag{2.19}
$$

Using the general concept of DFT (discrete Fourier Transform), a discrete signal $x(a)$ in the a domain with A points can be transformed into signal $X(b)$ in the b domain with period b by applying

$$
X(b) = \sum_{a=0}^{A-1} x(a)\, e^{-i\frac{2\pi}{A}a\cdot b}
\tag{2.20}
$$

Thereby, a DFT from the discrete time domain n to the k domain, as well as a DFT from the ramp domain l to the s domain can be applied. This is a two-dimensional Fourier transform

$$
s_{\mathrm{IF_a,2D}}(k,p) = A_{\mathrm{IF}}\, e^{i2\pi\frac{2f_c R}{c}} \left[\sum_{l=0}^{L-1} e^{i2\pi\left(\frac{2f_c vT_r}{c}\right)l} \left[\sum_{n=0}^{N-1} e^{i2\pi\left(\frac{2f_c v}{c}+\frac{2RB}{c\cdot T_c}\right)nT_s} e^{-i\frac{2\pi}{N}n\cdot k}\right] e^{-i\frac{2\pi}{L}l\cdot p}\right].
\tag{2.21}
$$

where, k is the beat frequency index, p is the Doppler frequency index, l is the chirp index, n is the sample index of the discrete signal, N is the number of samples (range gates) in the first Fourier transform and L is the number of samples in the second Fourier transform.

Remembering that the Discrete Time Fourier Transform of an exponential function $\mathrm{DTFT}\{e^{i\Omega_0 n}\} = 2\pi\delta(\Omega-\Omega_0)$ is an impulse located at Ω_0, it becomes clear that after applying the two dimensional Fourier transform the peaks appear at the positions

$$
\begin{aligned}
k &= \left(\frac{2f_\mathrm{c}v}{c} + \frac{2RB}{c \cdot T_\mathrm{c}}\right) T_\mathrm{s}\, N = f_\mathrm{B}\, T_\mathrm{s} N \\
&\approx \frac{2RB}{c \cdot T_\mathrm{c}}\, T_\mathrm{s} N = f_\mathrm{R}\, T_\mathrm{s} N
\end{aligned} \tag{2.22}
$$

$$
p = \frac{2f_\mathrm{c} v T_\mathrm{r}}{c}\, L = f_\mathrm{D}\, T_\mathrm{r} L. \tag{2.23}
$$

Hence, the range can be calculated taking the value of the range frequency f_R given by (2.22) and applying (2.15). Similarly, the velocity can be estimated using the value of the Doppler frequency f_D given by (2.23) and applying (2.8).

Fig. 2.5 show the graphical representation of the signal processing for a chirp-sequence modulation. The usual way to implement the algorithm is to perform a Fast Fourier Transform (FFT) for each single chirp over N samples in order to measure the target range R. Then, a second FFT is performed inside each single range gate over a sequence of L adjacent chirp signals.

The range frequency can be measured unambiguously inside the interval $[0, f_\mathrm{Rmax}]$. The maximum rage frequency f_Rmax results from the sampling theorem constraint [5]

$$
f_\mathrm{Rmax} = \frac{1}{2} f_\mathrm{s} = \frac{1}{2} \frac{1}{T_\mathrm{s}}. \tag{2.24}
$$

Then, using (2.15) the maximum range that can be measured is

$$
r_\mathrm{max} = \frac{cT_\mathrm{c}}{2B} f_\mathrm{Rmax} = \frac{cT_\mathrm{c}}{4B} f_\mathrm{s}. \tag{2.25}
$$

The ability to distinguish between close targets is given by the range resolution. It is worth mentioning that it is inversely proportional to the bandwidth B

$$
\Delta r = \frac{cT_\mathrm{c}}{2B} \Delta f_\mathrm{R} = \frac{cT_\mathrm{c}}{2B} \frac{1}{T_\mathrm{c}} = \frac{c}{2B}, \tag{2.26}
$$

$$
\Delta r \propto \frac{1}{B}. \tag{2.27}
$$

Similarly, the Doppler frequency can be measured unambiguously inside the interval $[0, f_\mathrm{Dmax}]$. The maximum Doppler frequency f_Dmax results from the sampling theorem constraint [5]

$$
f_\mathrm{Dmax} = \frac{1}{2} \frac{1}{T_\mathrm{r}}. \tag{2.28}
$$

Then, using (2.8) the maximum velocity is

$$
v_\mathrm{max} = \frac{c}{2f_\mathrm{c}} f_\mathrm{Dmax} = \frac{c}{4 f_\mathrm{c} T_\mathrm{r}}. \tag{2.29}
$$

The ability to distinguish between targets with similar velocity is given by the velocity resolution,

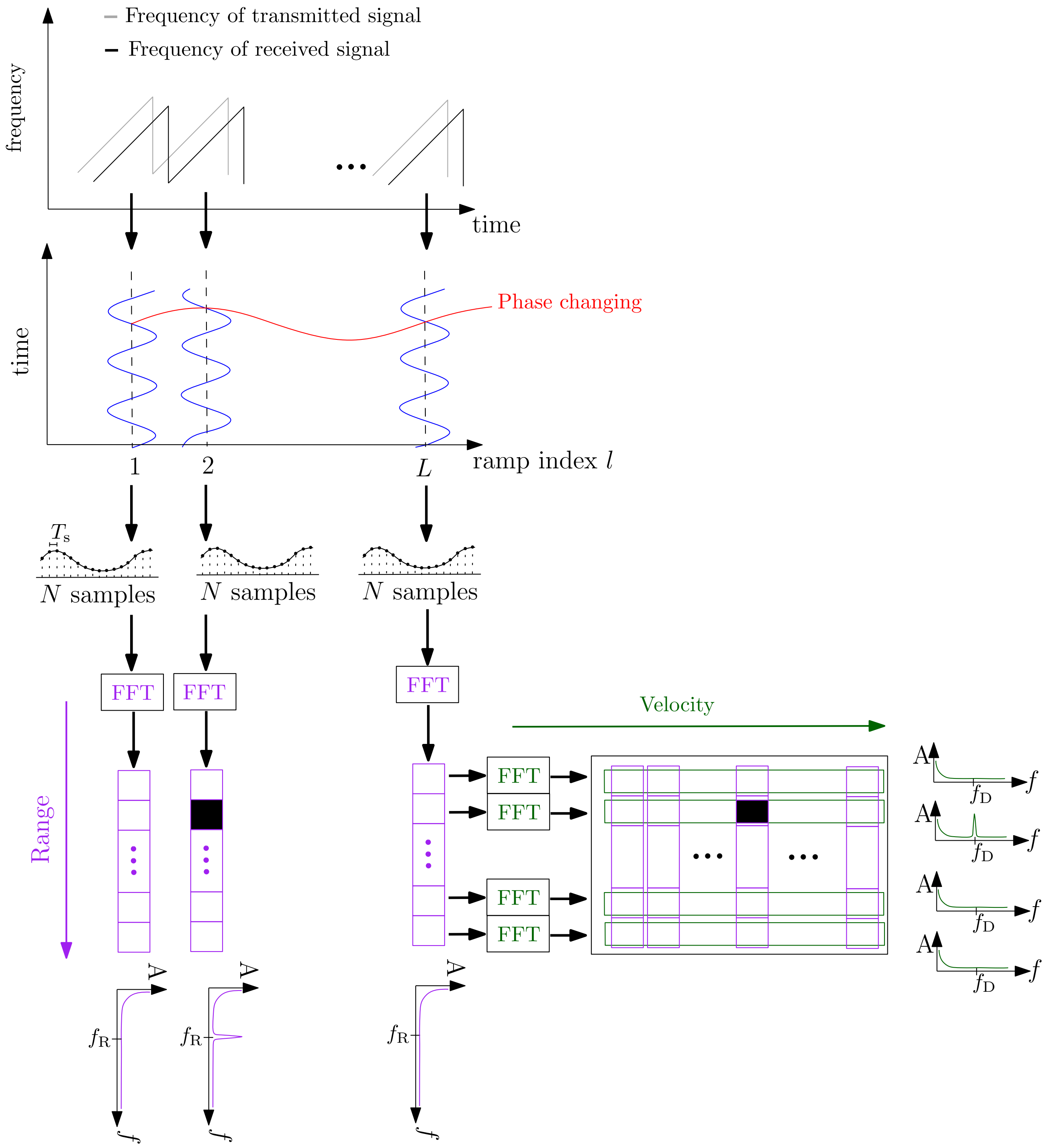

Fig. 2.5: Range and Velocity signal processing for consecutive chirps.

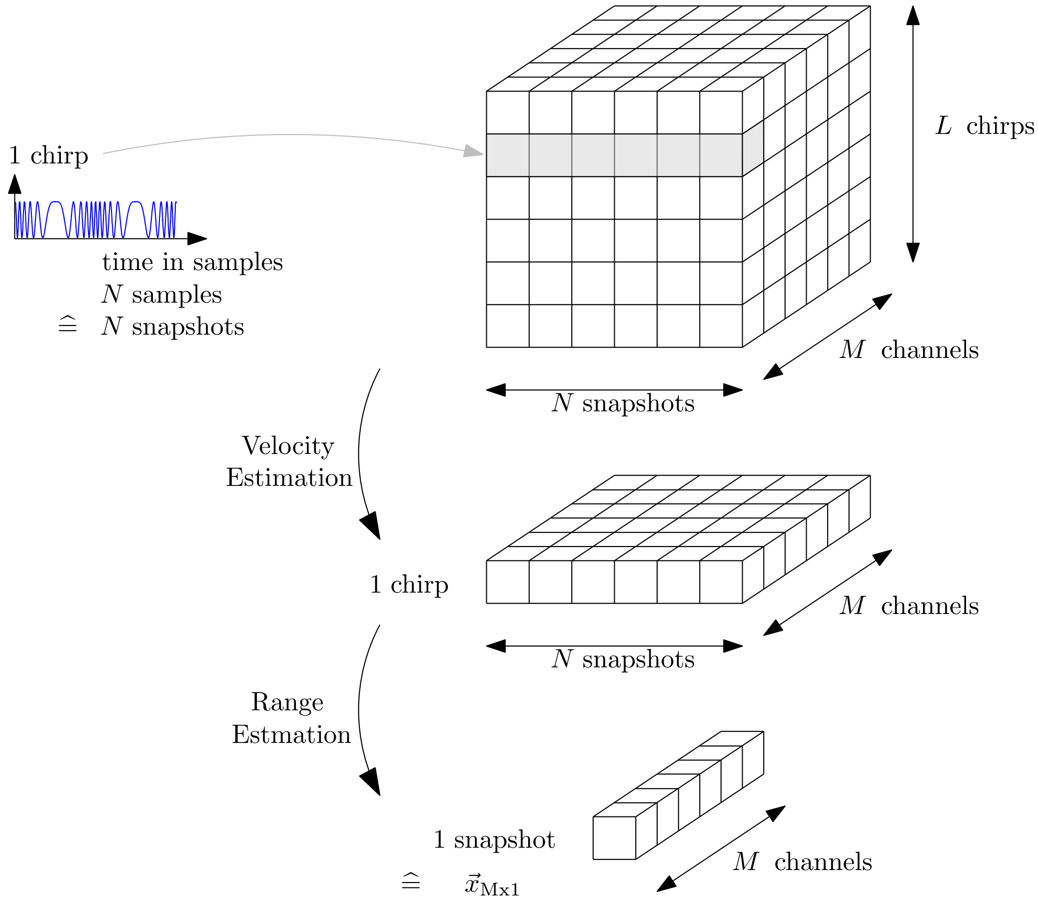

Fig. 2.6: 3-D Range and Velocity matrix signal processing including DOA estimation.

which is inversely proportional to the chirp repetition time T_{r}

$$\Delta v = \frac{c}{2f_{\mathrm{c}}}\Delta f_{\mathrm{D}} = \frac{c}{2f_{\mathrm{c}}}\frac{1}{T_{\mathrm{r}}L} = \frac{c}{2f_{\mathrm{c}}T_{\mathrm{r}}L}, \tag{2.30}$$

$$\Delta v \propto \frac{1}{T_{\mathrm{r}}}. \tag{2.31}$$

2.4 Overview of Signal Processing Chain

As was explained before (Fig. 2.1), after the echo signal arrives comes back to the target, it passes through a LNA, a LP filter and finally through an ADC converted. Later, the signal is processed in order to get the the velocity and range from the range-velocity 2-D matrix. Then, when M channels are available, M range-velocity matrices are obtained, and the range-velocity matrix 2-D matrix becomes 3-D. For this case the process to get the velocity and range of the targets is exactly the same, but, after applying the CFAR detection, the result is not a single range-velocity cell. For this case, the estimation of range and velocity leads in a single snapshot vector $\mathbf{x}_{\mathrm{Mx1}}$ with M positions. From this vector, the DOA estimation can be performed. Figure 2.6 shows the 3-D Range and Velocity matrix and the concept of snapshots.